PCCP

Fluorescence excitation spectrum of the 2-butoxyl radical and kinetics of its reactions with NO and NO_2

Ch. Lotz and R. Zellner

Institut für Physikalische und Theoretische Chemie, Universität Essen, D-45117 Essen, Germany

Received 19th February 2001, Accepted 1st May 2001
First published as an Advance Article on the web 11th June 2001

The ($\tilde{A} \leftarrow \tilde{X}$) fluorescence excitation spectrum of the 2-$C_4H_9O(\tilde{X})$ (2-butoxyl) radical in the wavelength range 345–390 nm was obtained using a combined laser photolysis/laser-induced fluorescence (LIF) technique following the generation of the radicals by excimer laser photolysis of 2-butylnitrite at $\lambda = 351$ nm. The fluorescence excitation spectrum shows 5 vibronic bands, where the dominant progression corresponds to the CO-stretching vibration in the first electronically excited state with $\tilde{\nu}'_{CO} = (560 \pm 10)$ cm^{-1}. The transition origin was assigned at $\tilde{\nu}_{00} = (26\,768 \pm 10)$ cm^{-1} ($\lambda_{00} = (373.58 \pm 0.15)$ nm). The kinetics of the reactions of the 2-butoxyl radical with NO and NO_2 at temperatures between $T = 223$–305 K and pressures between $p = 6.5$–104 mbar have been determined. The rate coefficients for both reactions were found to be independent of total pressure with $k_{NO} = (3.9 \pm 0.3) \times 10^{-11}$ cm^3 s^{-1} and $k_{NO_2} = (3.6 \pm 0.3) \times 10^{-11}$ cm^3 s^{-1} at $T = 295$ K. The Arrhenius expressions have been determined to be $k_{NO} = (9.1 \pm 2.7) \times 10^{-12} \exp((3.4 \pm 0.6)$ kJ mol$^{-1}/RT)$ cm^3 s^{-1} and $k_{NO_2} = (8.6 \pm 3.3) \times 10^{-12} \exp((3.3 \pm 0.8)$ kJ mol$^{-1}/RT)$ cm^3 s^{-1}. In addition, the radiative lifetime of the 2-$C_4H_9O(\tilde{A})$ radical after excitation at $\lambda = 365.938$ nm in the (0,1) band has been determined to be τ^{rad}(2-$C_4H_9O(\tilde{A})$) = (440 ± 80) ns. Quenching rate constants of the 2-$C_4H_9O(\tilde{A})$ radical were measured to be $k_q = (4.7 \pm 0.3) \times 10^{-10}$ cm^3 s^{-1} and $k_q = (5.0 \pm 0.4) \times 10^{-12}$ cm^3 s^{-1} for 2-butylnitrite and nitrogen, respectively.

1 Introduction

Alkoxyl radicals (RO) are key intermediates in the oxidative degradation of volatile organic compounds (VOCs) in the troposphere[1] as well as in hydrocarbon combustion chemistry. It is well known that alkoxyl radicals show four distinct competitive pathways under tropospheric conditions depending on their structure and environmental as well as exprimental conditions:[2] (i) reaction with O_2, yielding an aldehyde or a ketone and HO_2, (ii) unimolecular decomposition, forming an aldehyde and an alkyl radical, (iii) isomerization *via* an *n*-membered transition state (1,(n − 1)-H-shift; $n = 5$, 6) and (iv) recombination reaction with NO_x. While primary and secondary alkoxyl radicals up to C_3 mainly react with O_2, isomerization and unimolecular decomposition become more dominant with increasing number of carbon atoms. The reactions with NO and NO_2 may also become important for alkoxyl radicals in highly polluted environments, but are very important in the interpretation of smog chamber experiments due to the much higher concentrations of these gases. For the 2-butoxyl radical these reactions are schematically shown in Fig. 1. Note, however, that 2-butoxyl radicals cannot isomerize *via* a strain-free six-membered transition state. Hence isomerization in Fig. 1 is only shown for the sake of completeness.

From Fig. 1 it is obvious that while reactions with O_2 and NO_x are chain terminating, decomposition (and isomerization) lead to the formation of carbon centered radicals. These radicals are further oxidized, *i.e.* they rapidly add O_2 and react with NO to form another alkoxyl radical and NO_2. Hence the kinetics of these different possible reaction pathways have significant effects on the number of NO to NO_2 conversions that take place during the oxidation of the corresponding parent hydrocarbon. As NO_2 is easily photolysed, the branching ratio of alkoxyl radical reactions has a direct effect on the tropospheric production of ozone during photochemical smog episodes.

Although alkoxyl radicals represent a major branching point in the VOC oxidation schemes, only a few kinetic data are available in the literature. Our present understanding of their kinetics is mainly based on product yields and/or relative studies. Only a few direct studies[3–24] have been published, in which the highly sensitive LIF technique was used to detect the simplest alkoxyl radicals, methoxyl,[10–21] ethoxyl[5,19–23] and n-/iso-propoxyl.[5–7,24] The knowledge of the fluorescence excitation spectra of these radicals has been extremely useful for direct kinetic investigations. For a long time the lack of these spectra for higher ($\geqslant C_4$) alkoxyl radicals hindered direct kinetic studies on these radicals. In the last two years,

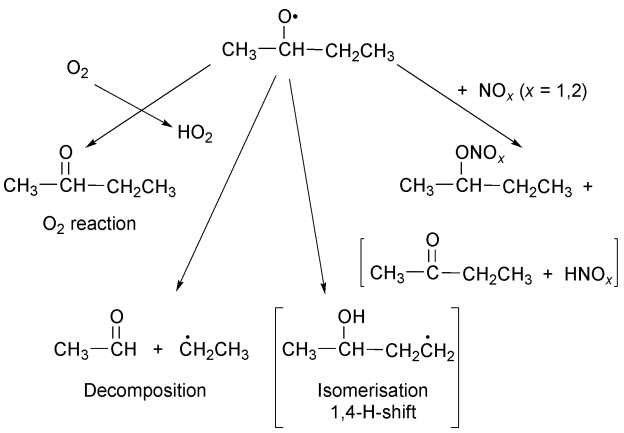

Fig. 1 Possible reactions of 2-butoxyl radicals under atmospheric conditions. The 1,4-H-shift isomerisation is only shown to illustrate an isomerisation pathway. Under atmospheric conditions it will not occur for 2-butoxyl.

however, several groups[3,4,25–27] have obtained fluorescence excitation spectra of the *tert*-butoxyl radical generated by laser photolysis of *tert*-butylnitrite at 351/355 nm or of di-*tert*-butylperoxide at 248 nm. Its unimolecular decomposition[3,25] as well as its reactions with NO[3,26] and NO_2[26] have been the subject of direct kinetic studies using the LIF technique. Even more recently, vibrationally resolved fluorescence excitation spectra have been obtained for 1-butoxyl,[27] 2-butoxyl,[3,27] 3-pentoxyl[28] and *tert*-pentoxyl.[28] Although these spectra provide a convenient tool for direct kinetic studies, there has been only one study by *Deng et al.*[29] in which the kinetics of the 2-butoxyl radical with O_2 and NO has been addressed.

In the present work we present the fluorescence excitation spectrum of 2-butoxyl radicals generated by the photolysis of 2-butylnitrite at 351 nm as well as results of direct temperature and pressure dependent measurements of the rate constants of the reaction of 2-butoxyl with NO and NO_2. To our knowledge this is the first direct study of the reaction of 2-butoxyl with NO_2.

2 Experimental

2-Butoxyl radicals were generated by the photolysis of 2-butylnitrite at 351 nm using the radiation from an excimer laser (Lambda Physik, LPX 105E). With a variable delay relative to the initial photolysis laser pulse the 2-butoxyl radicals were excited by an excimer laser pumped dye laser (Lambda Physik EMG 102 MSC, 308 nm (XeCl) and Lambda Physik FL2002). The relative concentration of these radicals was probed by monitoring the laser-induced fluorescence. Details of the experimental set-up have been described elsewhere[7,26] and only major aspects will be repeated here.

The experiments were performed under slow flow conditions in a stainless steel cell. The photolysis excimer laser beam and the probe excimer pumped dye laser beam pass coaxially but counterpropagating through this cell. In order to measure the relative pulse laser energies, reflections of the laser beams from the entrance windows of the cell were measured using pyroelectric energy meters (PEM 8, 245 and 310 V/J, Radiant Dyes). The fluorescence light is collected perpendicular to the main axis in the center of the cell by a system of lenses, passed through a cut-off filter (Schott GG 395/400 nm 3 mm) and is focussed onto the photocathode of the photomultiplier (Thorn EMI 9789 QB). The time dependent photomultiplier signal is integrated by a gated integrator/boxcar averager and fed into a personal computer. The delay time between the photolysis laser and the dye laser was variable within the range 5–8000 μs in steps of 5 μs.

The fluorescence excitation spectrum of 2-butoxyl was obtained by varying the wavelength of the dye laser in the range $\lambda = 345$–390 nm and detecting the integrated fluorescence intensity. In order to cover this wavelength range, DMQ and BiBuQ were used as laser dyes. The delay between the photolysis and dye laser shot was set to 10 μs. The dye laser step width and the scan frequency were 2.88×10^{-2} nm and 0.1 Hz, respectively, and lasers were operated with a repetition rate of 5 Hz. The signals were averaged over 25 pulses.

Kinetic investigations were performed with a repetition rate of 5 Hz. A typical 2-butoxyl decay curve consisted of 15–20 points corresponding to different delay times. The kinetic experiments were performed under pseudo-first order conditions with NO and NO_2 in at least 100 fold excess. For acquiring a fluorescence time profile the photomultiplier signal was averaged over 400 measurements.

The flow rates of the reactants were controlled using calibrated mass flow meters. The concentration of all gases in the cell were calculated from their mole fractions and the absolute pressure as determined by a capacitance manometer. 2-Butylnitrite was diluted in nitrogen ($x = 0.05$–0.08) and stored in 10 or 20 l glass bulbs in the dark. All other gases were taken from pressurized gas cylinders.

2-Butylnitrite was prepared by dropwise addition of concentrated sulfuric acid to a saturated solution of $NaNO_2$ and butan-2-ol.[30] 2-Butylnitrite appears as a pale yellow liquid, which was further purified by several freeze–pump–thaw cycles followed by trap to trap distillation. IR and UV spectra were used to verify the identity and purity of 2-butylnitrite.

Other gases and chemicals used had the following purities stated by the manufacturer (Messer Griesheim, if not otherwise stated): N_2, 99.999%; gas mixture NO, 99.8% in N_2, 99.999%; gas mixture NO_2, 98% in N_2, 99.999%. All gases were used without further purification.

3 Results and discussion

3.1 LIF detection of 2-butoxyl radicals

Fig. 2 shows the fluorescence excitation spectrum of 2-butoxyl ($\tilde{A} \leftarrow \tilde{X}$) at $T = 295$ K in the range 345–390 nm as obtained in the excimer laser photolysis at 351 nm of 1×10^{15} cm^{-3} 2-butylnitrite in 13 mbar nitrogen. The delay time between the photolysis laser pulse (<80 mJ pulse^{-1}) and the probe laser pulse (<8 mJ pulse^{-1}) was set to 10 μs. The spectrum was corrected for background and normalized for laser power variations. From the concentration of the photochemical precursor, an absorption cross section of $\sigma \approx 1.1 \times 10^{-19}$ cm^2 [31] at 351 nm, the photolysis laser fluence of 40 mJ cm^{-2} as well as an assumed quantum efficiency for RO–NO bond dissociation of one, the initial radical concentration can be estimated to be 8×10^{12} cm^{-3}.

Two different dyes were used to cover the scanning range. The spectra obtained with each dye showed the same structure in the overlapping region indicating that the peaks represent vibronic structure rather than noise. Therefore the spectra obtained with different dyes could be normalized to each other.

The fluorescence excitation spectrum of 2-butoxyl shows 5 intense vibronic bands. In analogy to the spectra of smaller alkoxyl radicals (CH_3O,[32–39] C_2H_5O,[40–43] n-/iso-C_3H_7O[6,7,43]) the dominant progression consisting of 3 bands can be assigned to the CO-stretching vibration in the electronically excited state with spacings of (560 ± 10) cm^{-1} and with the (0,0) band origin at 26 768 cm^{-1}. Two other intense vibrational bands, identified as peak a_1 and a_2 with a spacing of (614 ± 10) cm^{-1} and with a_1 located $\approx$311 cm^{-1} above the (0,0) band origin, are visible in Fig. 2. Since the spacing between these two peaks is clearly larger than that of the CO stretch progression, these peaks could either reflect an

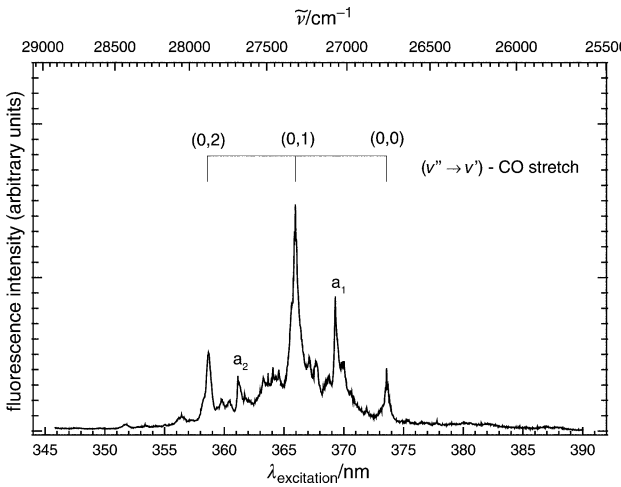

Fig. 2 ($\tilde{A} \leftarrow \tilde{X}$) fluorescence excitation spectrum of 2-butoxyl following the photolysis of 2-butylnitrite at $\lambda = 351$ nm. Pump to probe delay time: 10 μs, [2-C_4H_9ONO] = 1×10^{15} cm^{-3}, [2-$C_4H_9O(\tilde{X})$]$_i \approx 8 \times 10^{12}$ cm^{-3}, $p = 13$ mbar (nitrogen), $T = 295$ K.

unknown vibration or correspond to vibrational hot bands. All observed bands together with their vibrational band intervals are listed in Table 1.

The 2-butoxyl ($\tilde{A} \leftarrow \tilde{X}$) spectrum has recently been observed by Wang *et al.*[4] and Carter *et al.*,[27] who both generated the 2-butoxyl radicals in the 351 and 355 nm photolysis of 2-butylnitrite. Carter *et al.*[27] obtained the 2-butoxyl spectrum under jet-cooled conditions. The spectrum obtained in the present work is in good agreement with their studies as far as the positions of the observed bands is concerned. The values of 26 768 cm^{-1} and 560 cm^{-1} determined for the (0,0) transition and the CO-stretching frequency in the electronically excited state, respectively, agree excellently with those obtained by Carter *et al.*[27] (26 757 cm^{-1} and 559 cm^{-1}). Besides the CO fundamental stretch these authors observed three other cold bands and several vibrational hot bands. Peaks a_1 and a_2 in our spectrum may be identified as the "hot" vibrational band at $\approx$27 070 cm^{-1} and band b in Fig. 4 in ref. 27, respectively. In contrast Wang *et al.*[4] tentatively assigned the (0,0) transition at 26 185 cm^{-1}. This result, however, cannot be confirmed by our measurements. In fact, the authors have recently suggested reassigning the band origin of the 2-butoxyl spectrum to 26 774 cm^{-1} based on the trend for the origin frequencies of the different alkoxyl radicals.[28] However, their reported value for the CO-stretching frequency (567 cm^{-1}) agrees well with the present work. Additionally, analogues to peaks a_1 and a_2 in our spectrum can also be found in the 2-butoxyl spectrum obtained by Wang *et al.*[4]

Table 2 lists spectroscopic constants for alkoxyl radicals found in this work together with values from the literature. As can be seen the transition origin is shifted to lower wavenumbers with increasing size of the alkoxyl radical. The same observation is made when turning from primary to secondary as well as to tertiary radicals. The 1-butoxyl radical, the spectrum of which has been recently obtained by Carter *et al.*,[27] seems to be the only exception from this trend. Furthermore, the CO stretching frequency of the electronic ground state is always larger than that of the upper state, reflecting the increase of the C–O bond length during the electronic transition. The decrease of the CO stretching frequency from CH_3O to *tert*-C_4H_9O may reflect the increase of the reduced mass effect of the R_3C–O (R = H, CH_3, ...) moiety.

3.2 Lifetime and quenching behaviour of electronically excited 2-butoxyl

Studies of the quenching behaviour and the radiative lifetime of 2-butoxyl radicals were performed by exciting these radicals in the (0,1) band in the CO stretching progression at λ = 365.938 nm. N_2 and 2-butylnitrite were used as quenching partners, where the latter was applied as a mixture diluted in nitrogen.

A typical logarithmic fluorescence decay curve of electronically excited 2-butoxyl radicals as shown in Fig. 3 reflects single exponential behaviour. Stern–Volmer plots obtained for the decay constants of the fluorescence intensities in the presence of each collision partner are shown in Fig. 4. As

Table 1 Band assignments and positions in the fluorescence excitation spectrum of 2-butoxyl. Transitions in the dominant progression are assigned to CO-stretching vibrations ($v''_{CO} = 0$)

v'_{CO} =	0		1		2
$\tilde{\nu}$/cm^{-1}	26 768		27 327		27 887
$\Delta\tilde{\nu}$/cm^{-1}		559		560	
Peak:	a_1		a_2		
$\tilde{\nu}$/cm^{-1}	27 079		27 693		
$\Delta\tilde{\nu}$/cm^{-1}		614			

Table 2 Summary of spectroscopic properties of alkoxyl radicals

		$\tilde{\nu}_{CO\text{-}stretch}$/$cm^{-1}$		
Radical	$T_{00}(\tilde{A}–\tilde{X})$/$cm^{-1}$	$\tilde{X}$	$\tilde{A}$	Ref.
CH_3O	31 540	1015	678	35
	31 540	1022	683	43
	31 530	1020	670	44
	31 614.5	1047	660	33, 34
C_2H_5O	29 181	1060	603	41
	29 200	1080	600	44
	29 204	1067	596	40
n-C_3H_7O	28 637	1000	580	7
	29 000	1065	450	45
	28 634		582	27
i-C_3H_7O	27 167	900	560	7
	27 123		560	6
	27 140	960		45
	~27 167		560	43
	27 171		574,4	27
1-C_4H_9O	28 649			27
2-C_4H_9O	26 185		567	4
	26 768		560	This work
	26 757		559	27
tert-C_4H_9O	25 836		515	26
	25 866		521	4
	25 861		546	27
			500	3

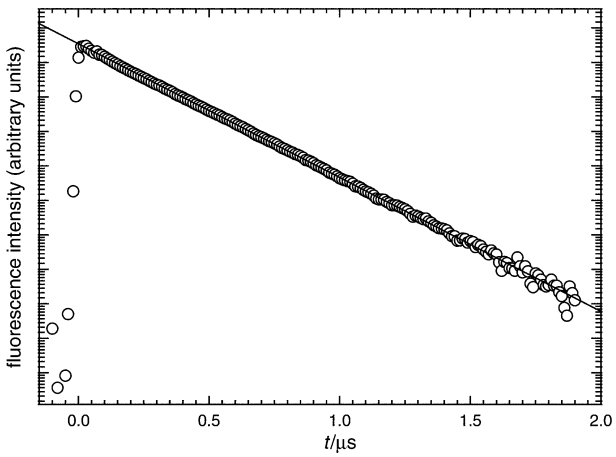

Fig. 3 Typical logarithmic decay curve of 2-$C_4H_9O(\tilde{A})$ fluorescence emission following the 351 nm photolysis of 2×10^{15} cm^{-3} 2-butylnitrite in the presence of 6.5 mbar nitrogen and excitation at 365.938 nm at T = 295 K. Pump to probe delay time: 10 μs.

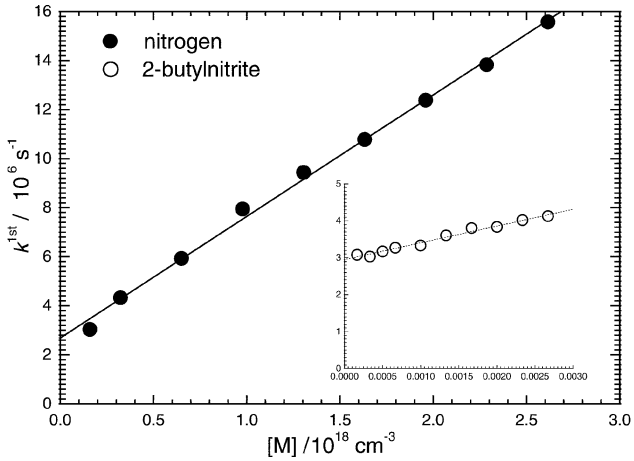

Fig. 4 Stern–Volmer plots for fluorescence quenching of 2-$C_4H_9O(\tilde{A})$ radicals with different collision partners at T = 295 K; 351 nm photolysis of 2-butylnitrite followed by excitation at 365.938 nm; pump to probe delay time: 10 μs; ●: [2-C_4H_9ONO] = 4×10^{15} cm^{-3}, variable total pressure; ○: [2-C_4H_9ONO] = variable, $p(N_2)$ = 6.5 mbar.

expected, the collisional quenching of 2-$C_4H_9O(\tilde{A})$ is particularly fast for 2-butylnitrite ($k = (4.7 \pm 0.3) \times 10^{-10}$ cm^3 s^{-1}). However, efficient quenching is also observed for 2-$C_4H_9O(\tilde{A})$ by nitrogen ($k = (5.0 \pm 0.4) \times 10^{-12}$ cm^3 s^{-1}). This contrasts with the quenching of electronically excited *tert*-butoxyl radicals by nitrogen, which has been found to be at least five hundred times slower ($k \leqslant 1 \times 10^{-14}$ cm^3 s^{-1})[26] and consequently negligible. This result, however, is not inconsistent with quenching efficiencies of nitrogen with other alkoxyl radicals.[7]

From the extrapolations of the individual Stern–Volmer plots to zero pressure a collision free lifetime of $\tau \approx (440 \pm 80)$ ns is derived. This value is close to those obtained for CH_3O ($\tau = 1.5$ μs[46]), for C_2H_5O ($\tau = 1.0$ μs[40]), for n- and iso-C_3H_7O ($\tau = 0.9$ μs[7] and 0.77 μs[5]) and for *tert*-C_4H_9O ($\tau = 1.5$ μs,[26] 1.0 μs[25] and 150 ns[4]). In contrast, Wang *et al.*[4] reported state specific lifetimes of electronically excited 2-butoxyl in the range 70–99 ns after excitation in three different vibrational bands ((0,1), (0,2) and a_1). The authors excluded the onset of predissociation as a reason for the slight mode-dependence of the fluorescence lifetime. Since in the present work 2-butoxyl radicals were only excited in the strongest (0, 1) band at $\lambda = 365.938$ nm, we are not able to extract a mode-dependence of the fluorescence lifetimes. However, similar discrepancies arose between Wang *et al.*'s[4] and our studies concerning the fluorescence lifetime of *tert*-butoxyl. In this case the larger value of the lifetime as obtained in our study[26] has recently been confirmed by Fittschen *et al.*[25]

3.3 The reaction of 2-butoxyl radicals with NO

Pseudo-first order rate constants k^{1st} for the reaction of 2-butoxyl radicals with NO were derived from the slope of the individual semi-logarithmic plots of the fluorescence intensities *vs.* the delay time between the photolysis and excitation laser. 2-Butoxyl radicals were excited at $\lambda = 365.938$ nm. In all cases the decays were found to be exponential and could be monitored over at least 3 lifetimes. Typical logarithmic decay curves at $T = 263$ K are shown in Fig. 5. In this case the NO concentration was varied in the range (0–2.2) $\times 10^{14}$ cm^{-3} with nitrogen as buffer gas and the initial 2-butoxyl radical concentration was estimated to be $\approx 4.5 \times 10^{11}$ cm^{-3}. k_{NO} can thus be obtained from the slope of a plot of k^{1st} *vs.* the reactant concentration. Typical examples for the reaction of 2-butoxyl with NO at different temperatures are shown in Fig. 6.

The intercepts reflect the sum of all removal processes other than the reaction with NO, namely diffusion out of the observation volume, unimolecular decomposition and the reaction with 2-butylnitrite as well as impurities. As can be seen from Fig. 6 the contribution of these processes to the intercept increases with temperature. Whereas diffusion is the main channel of loss at low temperatures in the absence of NO, unimolecular decomposition of 2-butoxyl becomes dominant at temperatures above $T = 253$ K ($k_0^{1st} > 800$ s^{-1}). The reaction of 2-butoxyl with 2-butylnitrite and its impurities (mainly NO_x) could be determined to be $k \approx (1–2) \times 10^{-12}$ cm^3 s^{-1} at $T = 295$ K. As a result the contribution of this process to the intercepts can be estimated to be small, especially at higher temperatures where the concentration of 2-butylnitrite (1.3×10^{14} cm^{-3}) in the present experiments is low. The rate coefficient for the unimolecular decomposition of 2-butoxyl will be presented in a forthcoming publication.[47]

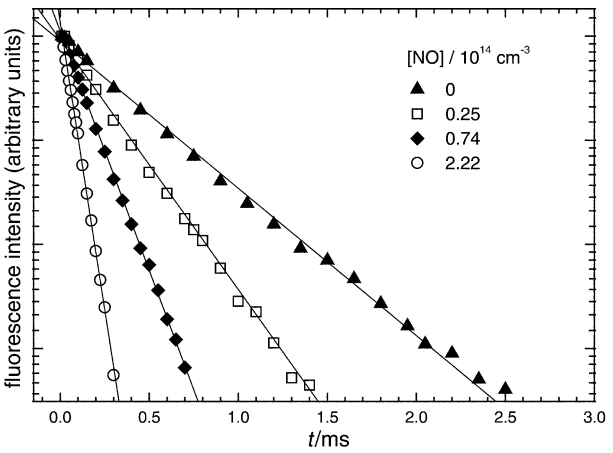

Fig. 5 Typical logarithmic 2-butoxyl decay traces following the 351 nm photolysis of 1.4×10^{14} cm^{-3} 2-butylnitrite in the presence of 26 mbar nitrogen and different concentrations of NO at 263 K, [2-$C_4H_9O(\tilde{X})]_i \approx 4.5 \times 10^{11}$ cm^{-3}.

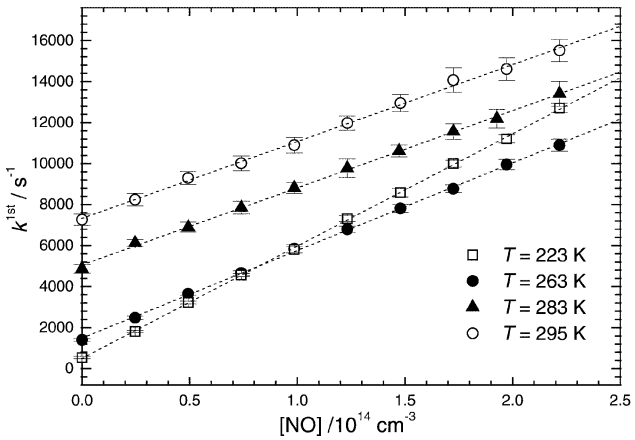

Fig. 6 Pseudo-first-order rate constant for the reaction of 2-butoxyl radicals with NO as a function of NO concentration at different temperatures. Buffer gas: N_2, $p = 26$ mbar, [2- C_4H_9ONO] $= 1.4 \times 10^{14}$ cm^{-3}, [2-$C_4H_9O(\tilde{X})]_i \approx 4.5 \times 10^{11}$ cm^{-3}.

Rate constants for the reaction of 2-butoxyl with NO were measured in the temperature range 223–305 K at $p = 26$ mbar and at 295 K in the range $p = 6.5$–104 mbar. The individual rate coefficients are listed in Table 3. The results of the pressure dependent measurements are summarized in Fig. 7. As can be seen, the data do not exhibit a significant pressure effect. As a result a rate coefficient at 295 K of $k_{NO,\,295\,K} = (3.9 \pm 0.3) \times 10^{-11}$ cm^3 s^{-1} is obtained. Fig. 8 shows the corresponding Arrhenius plot, from which the expression:

$$k_{NO} = (9.1 \pm 2.7) \times 10^{-12} \exp((3.4 \pm 0.6)\ \text{kJ mol}^{-1}/RT)\ \text{cm}^3\ \text{s}^{-1}$$

was derived.

Table 3 Summary of rate coefficients for the reactions (1) 2-C_4H_9O + NO → products, (2) 2-C_4H_9O + NO_2 → products for different temperatures, bath gas: N_2, $p = 26$ mbar[a]

T/K	$k_{NO}/10^{-11}$ cm^3 s^{-1}	$k_{NO_2}/10^{-11}$ cm^3 s^{-1}
223	5.48 ± 0.13	4.95 ± 0.22
233	5.20 ± 0.13	5.07 ± 0.29
243	4.96 ± 0.10	4.68 ± 0.22
253	4.60 ± 0.29	4.39 ± 0.25
263	4.27 ± 0.16	3.99 ± 0.20
273	3.92 ± 0.20	3.74 ± 0.25
283	3.76 ± 0.20	3.34 ± 0.24
295	3.86 ± 0.33	3.47 ± 0.23
305	3.10 ± 0.40	3.17 ± 0.47

[a] Limits represent statistical 2σ-errors. The systematic error can be estimated to be less than 30%.

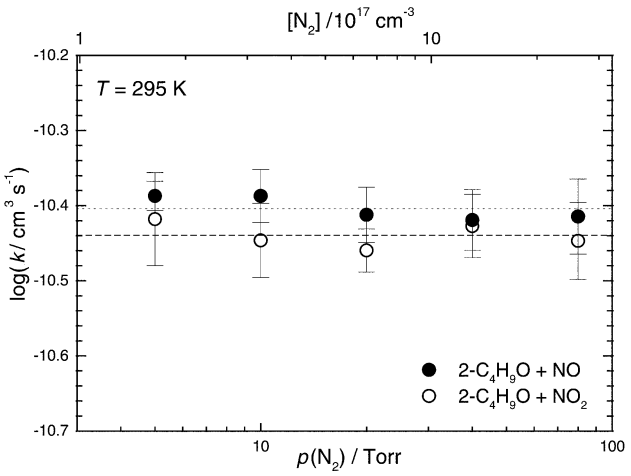

Fig. 7 Dependence of the second order rate constant for the reactions 2-C_4H_9O + NO → products and 2-C_4H_9O + NO_2 → products on total pressure. T = 295 K, buffer gas: N_2, [2-C_4H_9ONO] = 1.4 × 10^{14} cm^{-3}, [2-$C_4H_9O(\tilde{X})$]$_i$ ≈ 4.5 × 10^{11} cm^{-3}.

The rate coefficient for the reaction of 2-butoxyl radical with NO has previously been determined by Deng *et al.*[29] in the range T = 226–311 K using the laser photolysis/LIF technique and 2-butylnitrite as photochemical precursor. They reported pressure independent kinetics and an Arrhenius expression of $k_{NO} = (7.50 \pm 1.69) \times 10^{-12}$ exp((2.98 ± 0.47) kJ mol^{-1}/RT) cm^3 s^{-1}, in good agreement with the result obtained in the present work.

The reaction of primary and secondary alkoxyl radicals with NO may generally proceed *via* two channels,[31] namely

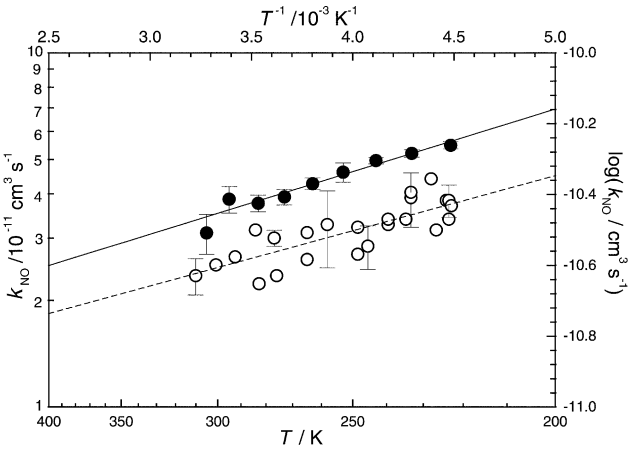

Fig. 8 Arrhenius representation of the rate coefficient of the reaction 2-C_4H_9O + NO → products, p_{tot} = 26 mbar (N_2); ●: this work, ○: Deng *et al.*[29]

(a) addition of NO and (b) abstraction of an α-hydrogen atom, *viz.*

$$CH_3CH(O^{\cdot})CH_2CH_3 + NO \xrightarrow{+M} CH_3CH(ONO)CH_2CH_3 \quad (1a)$$

$$\longrightarrow CH_3C(O)CH_2CH_3 + HNO \quad (1b)$$

In the present work no distinction between the two reaction channels can be made, since we only monitored 2-butoxyl radicals and hence the sum of the rate constants $k_1 = k_{1a} + k_{1b}$ was measured. Moreover, no attempts have been made to detect HNO as a reaction product in our experiments. The absence of any pressure effect also does not provide a hint as to which reaction channel is dominant. However, in analogy to the smaller alkoxyl radicals it can be supposed that the abstraction to addition ratio is very small and that the addition channel has reached its high pressure limit at pressures ⩽6.5 mbar.

The lack of a pressure dependence of the rate constant at room temperature is consistent with the results of former studies on the smaller alkoxyl radicals. As summarized in Table 4 the results of these studies on the reaction of alkoxyl radicals with NO show no pressure dependence for the rate constants above 15 mbar for all smaller alkoxyl radicals except methoxyl.

The slightly negative temperature dependence of the reaction of 2-butoxyl radicals with NO is indicative of a recombination reaction since collision complexes formed with higher internal energy are more likely to redissociate before stabilization.[49] Alternatively, the negative temperature dependence may be determined by the (temperature-dependent) capture rate constant as is common in barrierless recombination reactions.[50] The observed negative temperature dependencies seem to increase with increasing size of the alkoxyl radical. Atkinson's[2] recommendations for the reaction of all alkoxyl radicals with NO, as based on relative rate data (for methoxyl, ethoxyl, propoxyl, iso- and *tert*-butoxyl and *tert*-amyloxyl) cited by Batt[51] as well as direct kinetic studies on alkoxyl radicals ⩽ C_3, predict a slightly smaller temperature dependence but a higher A-factor for the reaction of 2-butoxyl with NO. Nevertheless our room temperature value for this reaction is very close to the predicted one. Hence Atkinson's[2] recommendation does not overestimate the rate coefficent for the reaction of NO with the 2-butoxyl radical at ambient temperatures, as was suggested for the corresponding reactions of the *tert*-butoxyl as well as higher alkoxyl radicals.[26]

3.4 The reaction of 2-butoxyl radicals with NO_2

Second order rate constants for the reaction of 2-butoxyl radicals with NO_2 were obtained as described above for the reaction with NO. Again, in all cases the 2-butoxyl decays were found to be exponential. The NO_2 concentration was varied

Table 4 Arrhenius parameters and k_{295} values of the reactions of alkoxyl radicals with NO from direct kinetic studies

Radical	$A/10^{-11}$ cm^3 s^{-1}	E_a/kJ mol^{-1}	$k_{295}/10^{-11}$ cm^3 s^{-1}	Ref.
CH_3O	—	—	3.6 ± 1	19
C_2H_5O	2.0 ± 0.7	−0.6 ± 0.4	3.88	5
n-C_3H_7O	1.2 ± 0.2	−2.9 ± 0.4	3.98	5
i-C_3H_7O	0.89 ± 0.02	−3.3 ± 0.5	3.3	5
	1.22 ± 0.28	−2.59 ± 0.59	3.28 ± 0.07	6
tert-C_4H_9O	0.76 ± 0.12	−3.2 ± 0.8	2.94 ± 0.11	26
	0.78 ± 0.18	−2.85 ± 0.29	2.5	3
2-C_4H_9O	0.750 ± 0.169	−2.98 ± 0.47	2.5 ± 0.9	29
	0.91 ± 0.27	−3.4 ± 0.6	3.86 ± 0.33	This work
All	2.3	−1.25	3.8	2, 48

in the range (0–2.2) × 10^{14} cm^{-3} with nitrogen as a buffer gas. The initial 2-butoxyl radical concentration was estimated to be 4 × 10^{11} cm^{-3}. The total pressure was varied in the range p = 6.5–104 mbar at T = 295 K. Fig. 7 summarizes the resulting rate coefficients for which no significant pressure effect could be observed. Consequently, a rate coefficient for the reaction of 2-butoxyl radicals with NO_2 at 295 K of $k_{NO_2,\,295\,K} = (3.6 \pm 0.3) \times 10^{-11}$ cm^3 s^{-1} is obtained.

Additionally, rate constants for the reaction of 2-butoxyl radicals with NO_2 were measured in the temperature range 223–305 K at p = 26 mbar. At low temperatures the dimerization of NO_2 to N_2O_4 had to be taken into account and the calculated NO_2 concentrations from the flow measurements had to be corrected for the NO_2/N_2O_4 equilibrium. The actual NO_2 concentration in the reaction cell corrected for equilibrium of dimerization was calculated from the expression:

$$[NO_2] = \frac{(\sqrt{8[NO_2]_0 K_{eq} + 1}) - 1}{4K_{eq}}, \qquad (2)$$

where $[NO_2]_0$ is the NO_2 concentration predicted from the flow measurement alone and K_{eq} [52] is the equilibrium constant. In order to verify if the flowing gas mixtures were given enough time to equilibrate before entering the observation volume in the cell, the linear gas velocity has been varied in the range 10–20 cm s^{-1}. No dependence of the measured first-order rate constant on this velocity, even at high NO_2 concentrations and low temperatures, could be observed.

Fig. 9 illustrates the effect of the dimerization equilibrium on the measured first-order rate constants. The solid points in this figure represent the first-order loss constant of 2-butoxyl radicals *vs.* $[NO_2]_0$. The open cycles are the first-order loss constant *vs.* the corrected NO_2 concentration given by eqn. (2). As can be seen there is a linear dependence between the first-order loss constant and the corrected NO_2 concentration. Hence, it can be concluded, that (i) N_2O_4 does not react as rapidly as NO_2 and (ii) the correction for N_2O_4 can be carried out quite accurately, since otherwise a non-linear dependence should be expected. It should be mentioned that this correction only had to be carried out for the temperatures 223 and 233 K.

An additional source of error includes the reaction of 2-butoxyl radicals with the photolysis products of NO_2, especially oxygen atoms. In order to exclude any secondary chemistry arising from NO_2 photolysis products, the excimer laser fluence was varied by at least a factor of two, but no influence on the measured first order rate constant at even the highest NO_2 concentrations was observed.

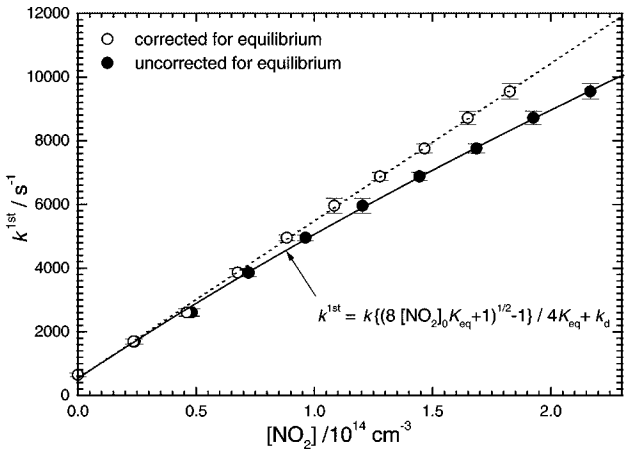

Fig. 9 Effect of the NO_2/N_2O_4 equilibrium at T = 223 K on the first-order 2-butoxyl loss constant. Solid points represent k^{1st} *vs.* $[NO_2]$ calculated from the gas flow outside the cell (*i.e.* uncorrected for the dimerization equilibrium). Open circles represent k^{1st} *vs.* $[NO_2]$ in the reactor after accounting for NO_2/N_2O_4 equilibrium. The solid line is a non-linear least square fit to the equation shown in the figure.

Fig. 10 shows the corresponding Arrhenius plot, from which the expression:

$$k_{NO_2} = (8.6 \pm 3.3) \times 10^{-12} \exp((3.3 \pm 0.8)\ \text{kJ mol}^{-1}/RT)\ \text{cm}^3\ \text{s}^{-1}$$

was obtained. The individual rate coefficients are listed in Table 3. Again, we observe a slightly negative temperature dependence, which is typical of a recombination reaction. To our knowledge this is the first direct study, in which the rate coefficient for the reaction of 2-butoxyl with NO_2 has been determined. Literature data are not available.

Similar to the reaction of 2-butoxyl with NO the reaction with NO_2 may proceed *via* two different reaction pathways, namely (a) addition of NO_2 and (b) abstraction of a β-hydrogen atom, *viz.*

$$CH_3CH(O^{\cdot})CH_2CH_3 + NO_2 \xrightarrow{+M} CH_3CH(ONO_2)CH_2CH_3 \qquad (3a)$$

$$\longrightarrow CH_3C(O)CH_2CH_3 + HNO_2 \qquad (3b)$$

For the same arguments as for the reaction of 2-butoxyl radicals with NO the addition channel (a) is considered to be the main reaction channel. Attempts to detect HONO have not been made.

Table 5 summarizes the results of earlier direct measurements on the reaction of smaller alkoxyl radicals with NO_2. Apart from methoxyl the high pressure limit for the reaction rate constant is reached far below 15 mbar for all other alkoxyl radicals. Hence, the lack of any pressure dependence of the rate of 2-butoxyl with NO_2 at room temperature as found in the present work is consistent with former studies on the smaller alkoxyl radicals. Unfortunately, the information on the temperature dependence of the reaction of alkoxyl radicals with NO_2 obtained in direct measurements and available in the literature is very limited. Only Balla *et al.*[6] reported an Arrhenius expression for the reaction of iso-propoxy with NO_2. These authors observed a dependence of the rate constant on photolysis energy, which they explained with the reaction of iso-propoxy, generated in the 351 nm photolysis of iso-propylnitrite, with $O(^3P)$. Therefore this Arrhenius expression was obtained from extrapolations of the observed rate constants to zero NO_2 photolysis at three different temperatures in the range 295–384 K. However, compared to iso-propoxyl the negative temperature dependence seems to increase for the reactions of *tert*- and 2-butoxyl with NO_2. The recommendations of Atkinson[48] for the reactions of all

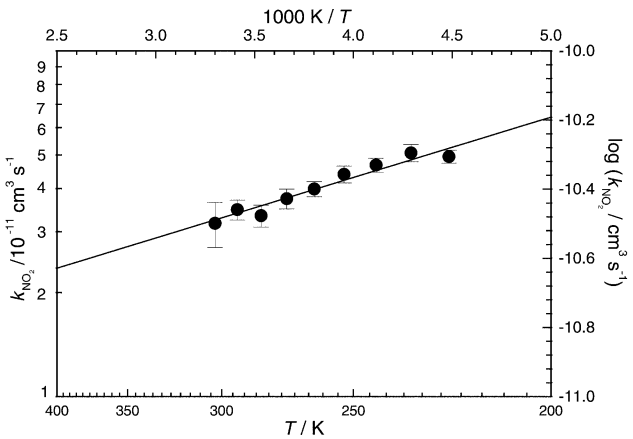

Fig. 10 Arrhenius representation of the rate coefficient of the reaction 2-C_4H_9O + NO_2 → products, p_{tot} = 26 mbar (N_2).

Table 5 Arrhenius parameters and k_{295} values of the reactions of alkoxyl radicals with NO_2 from direct kinetic studies

Radical	$A/10^{-11}$ cm^3 s^{-1}	E_a/kJ mol^{-1}	$k_{295}/10^{-11}$ cm^3 s^{-1}	Ref.
CH_3O	—	—	2.0 ± 0.4	20
C_2H_5O	—	—	2.8 ± 0.3	20
n-C_3H_7O	—	—	3.6 ± 0.4	7
i-C_3H_7O	—	—	3.3 ± 0.3	7
	1.48 ± 0.76	-2.18 ± 1.34	3.68 ± 0.16	6
tert-C_4H_9O	0.35 ± 0.12	-4.6 ± 0.7	2.42 ± 0.11	26
2-C_4H_9O	0.86 ± 0.33	-3.3 ± 0.8	3.47 ± 0.23	This work
All	2.3	-1.25	3.8	2, 48

alkoxyl radicals with NO_2, which are also listed in Table 5 and based on relative rate data (for methoxyl, ethoxyl and iso-propoxyl) cited by Batt,[51] again predict a smaller temperature dependence but a higher *A*-factor for the reaction of 2-butoxyl with NO_2. In contrast to *tert*-butoxyl our room temperature value for the reaction of 2-butoxyl with NO_2 is very close to the one predicted by Atkinson.

4 Summary and conclusions

LIF studies of the 2-butoxyl radical were performed and a fluorescence excitation spectrum was obtained following the 351 nm photolysis of 2-butylnitrite. Reaction rate constants of the 2-butoxyl radical with NO and NO_2 were measured as a function of temperature and pressure. Despite slightly negative dependencies on temperature in both cases no pressure dependence could be observed in the range 6.5–104 mbar at $T = 295$ K. Under most ambient tropospheric conditions the reactions of 2-butoxyl with NO and NO_2 are of minor importance compared to unimolecular decomposition and reaction with oxygen. The reactions with NO and NO_2 become only significant in highly polluted areas as well as in the interpretation of smog chamber experiments.

References

1 W. P. L. Carter and R. Atkinson, *J. Atmos. Chem.*, 1985, **3**, 377.
2 R. Atkinson, *Int. J. Chem. Kinet.*, 1997, **29**, 99.
3 M. Blitz, M. J. Pilling, S. H. Pilling and P. W. Seakins, *Phys. Chem. Chem. Phys.*, 1999, **1**, 73.
4 Ch. Wang, L. G. Shemesh, W. Deng, M. D. Lilien and T. S. Dibble, *J. Phys. Chem. A*, 1999, **103**, 8207.
5 C. Fittschen, A. Frenzel, K. Imrik and P. Devolder, *Int. J. Chem. Kinet.*, 1999, **31**, 1999.
6 R. J. Balla, H. H. Nelson and J. R. McDonald, *Chem. Phys.*, 1985, **99**, 323.
7 Ch. Mund, Ch. Fockenberg and R. Zellner, *Ber. Bunsen-Ges. Phys. Chem.*, 1998, **102**, 709.
8 H. Hein, A. Hoffmann and R. Zellner, *Ber. Bunsen-Ges. Phys. Chem.*, 1998, **102**, 1840.
9 H. Hein, A. Hoffmann and R. Zellner, *Phys. Chem. Chem. Phys.*, 1999, **1**, 3743.
10 C. Fittschen, B. Decroix, N. Gomez and P. Devolder, *J. Chim. Phys.*, 1998, **95**, 2129.
11 P. Biggs, C. E. Canosa-Mas, J.-M. Fracheboud, A. Douglas Parr, D. E. Shallcross, R. P. Wayne and F. Caralp, *J. Chem. Soc., Faraday Trans.*, 1993, **89**, 4163.
12 N. Sanders, J. E. Butler, L. R. Pasternack and J. R. McDonald, *Chem. Phys.*, 1980, **48**, 203.
13 A. Aranda, V. Daële, G. Le Bras and G. Poulet, *Int. J. Chem. Kinet.*, 1998, **30**, 249.
14 D. Rhäsa and R. Zellner, *Chem. Phys. Lett.*, 1986, **132**, 474.
15 K. Lorenz, D. Rhäsa, R. Zellner and B. Fritz, *Ber. Bunsen-Ges. Phys. Chem.*, 1985, **89**, 341.
16 P. J. Wantuck, R. C. Oldenborg, S. L. Baughcum and K. R. Winn, *J. Phys. Chem.*, 1987, **91**, 4653.
17 P. Biggs, C. E. Canosa-Mas, J.-M. Fracheboud, D. E. Shallcross and R. P. Wayne, *J. Chem. Soc., Faraday Trans.*, 1997, **93**, 2481.
18 F. Caralp, M.-T. Rayez, W. Forst, N. Gomez, B. Delcroix, Ch. Fittschen and P. Devolder, *J. Chem. Soc., Faraday Trans.*, 1998, **94**, 3321.
19 M. J. Frost and I. W. M. Smith, *J. Chem. Soc., Faraday Trans.*, 1990, **86**, 1757.
20 M. J. Frost and I. W. M. Smith, *J. Chem. Soc., Faraday Trans.*, 1990, **86**, 1751.
21 D. Gutman, N. Sanders and J. E. Butler, *J. Phys. Chem.*, 1982, **86**, 66.
22 D. Hartmann, J. Karthäuser, J. P. Sawerysyn and R. Zellner, *Ber. Bunsen-Ges. Phys. Chem.*, 1990, **94**, 639.
23 F. Caralp, P. Devolder, Ch. Fittschen, N. Gomez, H. Hippler, R. Méreau, M. T. Rayez, F. Striebel and B. Viskolcz, *Phys. Chem. Chem. Phys.*, 1999, **1**, 2935.
24 P. Devolder, Ch. Fittschen, A. Frenzel, H. Hippler, G. Poskrebyshev, F. Striebel and B. Viskolcz, *Phys. Chem. Chem. Phys.*, 1999, **1**, 675.
25 Ch. Fittschen, H. Hippler and B. Viskolcz, *Phys. Chem. Chem. Phys.*, 2000, **2**, 1677.
26 Ch. Lotz and R. Zellner, *Phys. Chem. Chem. Phys.*, 2000, **2**, 2353.
27 C. C. Carter, J. R. Atwell, S. Gopalakrishnan and T. A. Miller, *J. Phys. Chem. A*, 2000, **104**, 9165.
28 Ch. Wang, W. Deng, G. G. Shemesh, M. D. Lilien, D. R. Katz and T. S. Dibble, *J. Phys. Chem. A*, 2000, **104**, 10368.
29 W. Deng, Ch. Wang, D. R. Katz, G. R. Gawinski, A. J. Davis and T. S. Dibble, *Chem. Phys. Lett.*, 2000, **330**, 541.
30 A. H. Blatt, *Organic Syntheses*, Collective Volume 2, Wiley, New York, 1943.
31 J. Heicklen, *Adv. Photochem.*, 1988, **14**, 177.
32 H. R. Wendt and H. E. Hunziker, *J. Chem. Phys.*, 1979, **71**, 5202.
33 St. C. Foster, P. Misra, T. D. Lin, C. P. Damo, Ch. C. Carter and T. A. Miller, *J. Phys. Chem.*, 1988, **92**, 5914.
34 X. Liu, C. P. Damo, T. D. Lin, St. C. Foster, P. Misra, L. Yu and T. A. Miller, *J. Phys. Chem.*, 1989, **93**, 2266.
35 G. Inoue, H. Akimoto and M. Okuda, *J. Chem. Phys.*, 1980, **72**, 1769.
36 P. Misra, X. Zhu, Ch.-Y. Hsueh and J. B. Halpern, *Chem. Phys.*, 1993, **178**, 377.
37 P. Misra, X. Zhu and A. H. Nur, *Spectrosc. Lett.*, 1992, **25**, 639.
38 K. Fuke, K. Ozawa and K. Kaya, *Chem. Phys. Lett.*, 1986, **126**, 119.
39 D. E. Powers, M. B. Pushkarsky and T. A. Miller, *J. Chem. Phys.*, 1997, **106**, 6863.
40 G. Inoue, M. Okuda and H. Akimoto, *J. Chem. Phys.*, 1981, **75**, 2060.
41 X. Zhu, M. M. Kamal and P. Misra, *Pure Appl. Opt.*, 1996, **5**, 1021.
42 X. Q. Tan, J. M. Williamson, St. C. Foster and T. A. Miller, *J. Phys. Chem.*, 1993, **97**, 9311.
43 St. C. Foster, Y.-Ch. Hsu, C.-P. Damo, X. Liu, Ch.-Yi Kung and T. A. Miller, *J. Phys. Chem.*, 1986, **90**, 6766.
44 T. Ebata, H. Yanagishita, K. Obi and I. Tanaka, *Chem. Phys.*, 1982, **69**, 27.
45 J. Bai, H. Okabe and M. K. Emadi-Babaki, *J. Photochem. Photobiol. A*, 1989, **50**, 163.
46 G. Inoue, H. Akimoto and M. Okuda, *Chem. Phys. Lett.*, 1979, **63**, 213.
47 Ch. Lotz, H. Somnitz and R. Zellner, to be published.
48 R. Atkinson, *J. Phys. Chem. Ref. Data*, 1997, **26**, 232.
49 M. J. Pilling and P. W. Seakins, *Reaction Kinetics*, Oxford University Press, 1995.
50 J. Troe, *J. Chem. Soc., Faraday Trans.*, 1994, **90**, 2303.
51 L. Batt, *Int. Rev. Phys. Chem.*, 1987, **6**, 53.
52 W. B. Moore, S. P. Sander, D. M. Golden, R. F. Hampson, M. J. Kurylo, A. R. Ravishankara, C. E. Kolb and M. J. Molina, *Chemical Kinetics and Photochemical Data for Use in Stratospheric Modelling*, Jet Propulsion Lab., Pasadena, CA, 1997, JPL Pub. 97-4.